Nuclear Data for Science and Technology (1988 MITO), 1121-1124, Copyright © 1988 JAERI.

CALCULATED PROTON-INDUCED THICK-TARGET RADIONUCLIDE ACTIVATION YIELDS AND NEUTRON YIELD SPECTRA FOR $E_p \leq 50$ MeV, WITH COMPARISONS TO OTHER CALCULATIONS AND MEASURED DATA

W. B. Wilson, E. D. Arthur, R. J. LaBauve and R. T. Perry
Los Alamos National Laboratory, Los Alamos, New Mexico, USA 87545

Abstract: Radionuclide production cross sections have been calculated with the GNASH code for protons below 50 MeV incident of on the stable nuclides of a range of elements common to accelerator materials. These elements include C, O, Ne, Al, Si, Fe, Co, Ni, Cu, and W. These data, augmented with limited measured data, have been used with the proton stopping cross-section data of Anderson and Ziegler to calculate thick-target yield values for the formation of a range of radionuclides in accelerator materials. Illustrative results are presented. GNASH calculations have also been made on a grid of proton energies below 50 MeV to produce differential cross sections describing angle-integrated neutron production spectra. The angular distribution systematics of Kalbach and Mann have been used to produce double-differential cross-section, which were used with the proton stopping data to produce anisotropic thick-target neutron yield spectra. Results are presented for 52-MeV protons on a thick target of Cu. Comparisons are made with results of HETC calculations, using cross sections from the intranuclear cascade plus evaporation model, and with thick-target neutron yield spectra measured by Nakamura, Fujii, and Shin.

(accelerators, medium-energy protons, proton activation, thick-target neutron yields)

Introduction

Shield requirements for particle accelerators are generally determined by the neutron source produced by the particles interacting on target materials. Residual activation of the accelerator and its environment is produced by the beam spilling on accelerator components or targets and by neutron reactions on all materials within the containment. The thick-target anisotropic neutron source spectra produced by beam particles on accelerator materials are available for few combinations of particle type, particle energy, target nuclide, and emission angle. Similarly, thick-target radionuclide yields are largely unknown. These can be calculated in thick-target continuous slowing down calculations using particle energy-dependent radionuclide production cross sections and double-differential neutron production cross sections. We have used cross sections from nuclear reaction physics model code calculations, angular distribution systematics, and proton slowing data to obtain thick target yields. These data and calculations are described in the sections that follow.

GNASH Calculations

GNASH,[1] a preequilibrium statistical nuclear model code, was used for producing the composite spectra and individual reaction data for reactions on the major stable nuclides of C, O, Ne, Al, Si, Fe, Co, Ni, Cu and W. In addition to the use of standard Hauser-Feshbach formalisms, the GNASH code was modified to include an evaporation model[2] and s-wave model[3,4] for use at higher energies, typically greater than 36 MeV. These two models include a new expression for neutron-proton yield ratios for preequilibrium particle emission and also include implementation of a multistage preequilibrium model.[5] Finally, a Gilbert Cameron level density model was used to describe continuum excitation energy regions. Composite systems formed were allowed to decay by γ, neutron, proton, deuteron and α emission. At lower energies typically 10 to 12 compound nuclei were formed and allowed to decay. At higher energies, for the heavier elements, as many as 42 compound nuclei were allowed to be formed and decay.

Values of input parameters used in most calculations were defaults determined from previous calculations. These included values used for normalization of phenomenological matrix element expressions used to calculate preequilibrium emission as well as gamma-ray strength functions which served to normalize gamma-ray competition to particle emission. Finally, particle transmission coefficients and inverse reaction cross sections were determined from spherical optical model calculations which employed new potentials developed by Madland[6,7] for use at higher energies.

Cross sections leading to each of the particles and residual nuclides were accumulated from all reaction paths leading to the product using a utility code READGN. A typical result is the $^{27}Al(p,x)^{18}F$ cross section shown in figure 1, where the calculated cross section compares well with the measured data of Hintz[8,9] and Williams and Fulmer.[10] Not typical, however, is the existence of measured data to establish the uncertainty of calculated reaction cross sections; we assume that cross section values are generally accurate to perhaps a factor of two.

Thick Target Yields

Thick-target yield values are calculated as the integral over proton energy, from reaction threshold to initial proton energy, of the ratio of reaction cross section to stopping cross section.[11] Reaction cross sections for the production of each product for each target nuclide have been tabulated in a data file for these thick target calculations, which use the functional proton stopping cross sections of Anderson and Ziegler.[12] The ingredients of the p+Al thick target neutron yield calculation, as well as the calculated result, are shown in figure 2. Also shown are the measured neutron yield data of Tai et al.,[13] with which the calculated values agree very well.

Thick Target Yield Spectra

Thick target neutron yield spectra are calculated in a manner similar to thick target yield calculations, using double differential neutron production cross sections describing the probability of neutron production at E_n and direction Ω. GNASH produces differential cross sections in the center- of-mass system describing the angle-integrated neutron production spectrum. The emission-particle angular distribution systematics of Kalbach and Mann[14] were used to superimpose the angular dependence upon the differential cross sections of GNASH, yielding double-differential cross sections. Such double-differential cross sections have been calculated for the neutron production from protons on Cu. These have been used to calculate the thick-target neutron yield spectrum produced by 52 MeV protons incident on a thick Cu target. The result at a laboratory angle of 15° is shown in figure 3, where it is compared with that measured by Nakamura et al.[15]. Also shown is the thick-target neutron yield spectrum calculated with the HETC code, which predicts a higher yield magnitude and harder neutron spectrum in this problem than the measured data or yield spectrum calculated with GNASH cross sections and Kalbach-Mann systematics.

Conclusions

Thick-target yields for nuclides produced by proton activation of several accelerator materials have been presented. The validity of GNASH calculated cross sections has been demonstrated with comparisons to measured cross sections, thick target yields and thick target neutron yield spectra. A comprehensive document listing both angle-integrated and angle-dependent thick target neutron yield spectra is in preperation.

References

1. P.G. Young and E.D. Arthur: LA-6947(1977).
2. E.D. Arthur and C. Kalbach: in LA-10915-PR(1986),pp 6-12.
3. M. Blann and M. Beckerman: *Nucleonika* 23,1(1978).
4. E.D. Arthur et al.: LA-UR-87-3383(1987)[Beijing 10/87]
5. E.D. Arthur: LA-10689-PR(1985),pp 8-30.
6. D.G. Madland: LA-UR-87-3382(1987).[Beijing 10/87]
7. D.G. Madland: LA-UR-88-376(1988).[Mito 5/88]
8. N.M. Hintz: *Phys. Rev.* 83,185 (1951).
9. N.M. Hintz and N.F. Ramsey: *Phys. Rev.* 88,19 (1952).
10. I. R. Williams and C. B. Fulmer, *Phys. Rev.* 162, 1055 (1967).
11. W.B. Wilson: this conference.
12. H.H. Anderson and J.F. Ziegler: *Hydrogen Stopping Powers and Ranges in All Elements,* Pergamon Press, NY (1977).
13. Y. Tai et al.: *Phys. Rev.* 109,2086 (1958).
14. C. Kalbach and F. Mann: *Phys. Rev.* C23,112 (1981).
15. T. Nakamura, M. Fujii and K. Shin, *Nucl. Sci.* 83,444 (1983).

Table 1. Calculated Thick Target Yields

product	Incident Proton Energy 30MeV	40MeV	50MeV
p + CARBON			
neut	6.00-4	2.34-3	5.89-3
H-02	5.88-4	1.40-3	3.98-3
He-02	0.	8.6-14	1.06-6
He-03	0.	2.04-5	2.56-4
He-04	1.52-2	3.48-2	5.46-2
He-05	0.	2.1-14	7.95-7
He-06	0.	3.9-15	4.45-8
Li-04	0.	3.96-8	1.31-5
Li-05	1.49-3	3.89-3	5.32-3
Li-06	0.	1.63-5	4.10-4
Li-07	1.17-6	2.23-4	1.22-3
Be-06	0.	7.9-12	9.09-7
Be-07*	9.78-6	5.15-4	1.28-3
Be-08	3.46-3	4.89-3	6.10-3
Be-09	0.	1.45-6	5.04-5
Be-10	3.3-11	1.33-6	1.68-5
B-07	0.	0.	1.69-8
B-08	8.38-8	3.14-5	1.65-4
B-09	1.42-3	2.10-3	2.73-3
B-10	2.69-6	3.63-4	1.61-3
B-11	8.55-4	1.91-3	3.09-3
C-10	0.	3.48-6	4.78-5
C-11*	1.58-3	4.61-3	8.37-3
N-11	0.	3.74-8	2.14-6
p + OXYGEN			
neut	4.43-4	1.86-3	4.53-3
H-02	7.82-4	2.81-3	6.50-3
H-03	1.98-5	1.58-4	4.99-4
He-04	6.26-3	1.13-2	1.70-2
Li-05	5.5-11	1.97-6	1.28-5
Li-07	0.	1.1-13	1.94-6
Be-06	0.	9.2-18	8.2-11
Be-07	0.	3.2-10	1.42-5
Be-08	4.65-5	2.92-4	8.23-4
Be-09	0.	0.	4.19-8
Be-10	0.	3.5-10	1.33-6
B-07	0.	0.	6.4-19
B-08	0.	7.1-14	6.61-7
B-09	1.63-5	6.49-5	1.17-4
B-10	0.	2.0-13	5.67-6
B-11	1.01-7	4.82-5	2.55-4
B-12	0.	0.	2.4-15
B-13	0.	0.	6.1-11
C-10	0.	4.1-11	1.31-5
C-11	4.59-9	1.51-4	6.78-4
C-12	4.06-3	8.38-3	1.21-2
C-13	0.	2.35-5	2.04-4
C-14	3.33-6	7.48-5	2.42-4
N-11	0.	0.	3.04-8
N-12	5.5-10	2.92-5	1.27-4
N-13	2.23-3	2.40-3	2.65-3
N-14	2.30-4	1.56-3	4.05-3
N-15	5.21-4	1.42-3	2.34-3
O-13	0.	0.	1.8-15
O-14	8.38-7	1.06-4	3.65-4
O-15	9.11-4	2.46-3	4.02-3
F-15	0.	1.16-6	6.44-6
p + NEON			
neut	8.36-4	2.30-3	4.74-3
H-02	7.02-4	2.34-3	5.16-3
H-03	3.45-5	1.41-4	4.18-4
He-04	8.75-3	1.54-2	2.37-2
B-09	1.98-9	1.37-6	9.71-6
B-10	2.1-10	9.61-9	5.22-8
B-11	4.34-8	8.11-7	9.73-6
B-12	0.	2.4-11	5.41-9
B-13	0.	2.5-16	9.4-10
C-10	0.	1.2-11	4.46-7
C-11	3.1-13	5.69-7	2.13-5
C-12	5.28-5	4.59-4	1.21-3
C-13	8.30-8	4.22-6	2.60-5
C-14	7.11-6	4.83-5	1.46-4
C-15	0.	1.1-11	6.16-9
C-16	0.	0.	6.89-9
N-11	0.	0.	1.4-15
N-12	0.	1.31-7	7.27-6
N-13	1.61-4	2.76-4	3.94-4
N-14	1.07-5	1.42-4	6.70-4
N-15	2.02-4	6.31-4	1.29-3
N-16	1.99-8	1.55-6	1.57-5
N-17	5.38-9	1.32-6	6.59-6
N-18	0.	0.	1.2-12
N-19	0.	0.	1.2-12
O-14	7.61-8	1.52-5	7.07-5
O-15	3.39-4	1.51-3	3.35-3
O-16	7.12-3	1.07-2	1.39-2
O-17	3.83-5	1.88-4	5.01-4
O-18	1.34-4	2.81-4	4.78-4
O-19	7.9-10	2.47-8	3.78-7
O-20	8.36-9	4.54-7	1.57-6
F-15	0.	6.2-10	8.81-7

product	Incident Proton Energy 30MeV	40MeV	50MeV
p + NEON (Continued)			
F-16	9.54-6	7.02-5	1.51-4
F-17	1.15-4	1.28-4	1.67-4
F-18	8.34-5	3.78-4	8.05-4
F-19	4.25-4	6.39-4	8.14-4
F-20	1.22-6	1.06-5	2.68-5
F-21	2.95-6	8.09-6	1.34-5
Ne-17	0.	0.	1.64-7
Ne-18	2.38-6	3.71-5	1.08-4
Ne-19	4.04-4	9.54-4	1.49-3
Na-19	0.	9.66-7	3.39-6
Na-20	1.82-9	1.27-8	5.78-8
Na-21	7.16-6	1.49-5	2.01-5
p + ALUMINUM			
neut	4.06-3	1.05-2	1.93-2
H-02	8.98-4	2.20-3	4.07-3
H-03	0.	0.	4.1-11
He-04	5.70-3	8.36-3	1.16-2
N-13	0.	4.51-9	4.91-7
N-14	0.	1.36-6	1.20-5
N-15	2.42-6	2.94-5	9.61-5
N-16	0.	0.	1.2-13
N-17	0.	0.	1.47-9
O-14	0.	0.	1.0-14
O-15	2.1-14	1.30-7	5.09-6
O-16	3.94-5	1.51-4	3.62-4
O-17	0.	7.21-9	1.07-5
O-18	1.8-15	8.17-9	6.13-6
O-20	0.	0.	1.4-16
F-17	0.	4.32-9	3.63-6
F-18	5.0-14	2.91-7	2.35-5
F-19	3.17-8	1.21-5	7.46-5
F-20	0.	0.	6.92-8
F-21	0.	2.8-10	1.56-6
Ne-18	0.	6.0-15	5.48-8
Ne-19	4.6-10	1.34-6	9.92-6
Ne-20	3.50-4	4.97-4	6.16-4
Ne-21	1.1-11	2.93-5	2.44-4
Ne-22	3.03-5	2.94-4	7.13-4
Ne-23	0.	0.	3.57-8
Ne-24	0.	6.9-12	1.79-7
Na-20	0.	0.	5.10-9
Na-21	8.0-10	1.05-5	8.32-5
Na-22	3.25-5	4.59-4	1.48-3
Na-23	1.46-3	2.58-3	3.36-3
Na-24	0.	5.99-6	8.89-5
Na-25	1.19-6	2.22-5	6.74-5
Mg-21	0.	0.	2.5-14
Mg-22	8.8-14	6.12-7	5.08-6
Mg-23	8.89-5	2.51-4	3.89-4
Mg-24	3.28-3	3.52-3	3.99-3
Mg-25	8.05-4	2.87-3	5.02-3
Mg-26	3.28-3	4.89-3	6.07-3
Al-23	0.	0.	4.7-13
Al-24	0.	1.25-7	2.52-6
Al-25	4.79-5	3.67-4	8.36-4
Al-26	2.01-3	3.48-3	4.68-3
Si-25	0.	6.3-11	5.63-8
Si-26	1.16-5	3.71-5	5.94-5
p + SILICON			
neut	4.86-4	1.71-3	3.88-3
H-02	1.79-4	7.70-4	1.79-3
He-04	2.59-3	4.88-3	8.50-3
O-14	0.	0.	8.1-13
O-15	0.	3.20-8	3.18-6
O-16	1.08-5	1.11-4	3.51-4
O-17	0.	0.	6.82-8
O-18	0.	0.	2.02-7
F-16	0.	0.	2.2-16
F-17	3.1-15	6.25-8	2.40-6
F-18	0.	0.	7.5-13
F-19	0.	2.1-12	1.96-6
F-21	0.	0.	2.2-23
Ne-18	0.	0.	2.0-21
Ne-19	0.	4.3-15	7.65-7
Ne-20	4.01-6	2.07-4	8.49-4
Ne-21	0.	6.5-22	3.59-8
Ne-22	0.	1.46-8	1.73-5
Ne-24	0.	0.	1.4-21
Na-19	0.	0.	2.2-24
Na-20	0.	7.9-15	3.87-7
Na-21	2.26-6	1.48-5	2.42-5
Na-22	0.	2.63-8	2.75-5
Na-23	2.73-6	2.48-4	1.04-3
Na-24	0.	0.	1.6-10
Na-25	0.	5.4-14	5.32-8
Mg-22	0.	9.2-17	3.89-8
Mg-23	4.81-8	2.40-5	1.91-4
Mg-24	2.36-3	3.93-3	5.23-3
Mg-25	8.3-15	2.16-5	3.91-4
Mg-26	7.25-5	9.74-4	1.78-3
Al-23	0.	0.	1.88-8

product	Incident Proton Energy 30MeV	40MeV	50MeV
p + SILICON (Continued)			
Al-24	8.76-8	6.40-6	2.19-5
Al-25	2.21-4	2.24-4	2.40-4
Al-26	3.11-5	7.70-4	2.23-3
Al-27	5.16-3	8.34-3	1.04-2
Si-25	0.	0.	4.6-18
Si-26	2.28-9	3.05-6	2.73-5
Si-27	5.88-4	1.58-3	2.60-3
P-27	0.	7.63-7	5.51-6
p + IRON			
neut	8.19-3	1.63-2	2.63-2
H-02	2.99-4	8.49-4	1.65-3
He-04	9.43-4	2.03-3	3.59-3
Sc-47	0.	1.5-34	7.5-18
Ti-47	3.9-28	7.5-13	2.80-7
Ti-48	2.1-11	2.45-7	7.76-6
V-46	1.5-21	5.5-11	7.30-8
V-47	2.64-7	2.53-6	8.05-6
V-48	9.7-13	6.65-7	3.11-5
V-49	3.29-6	4.54-5	1.46-4
V-50	5.2-20	1.43-7	4.48-5
V-51	2.04-7	2.61-5	1.32-4
Cr-48	0.	1.3-10	1.00-6
Cr-49	6.37-8	1.42-5	6.10-5
Cr-50	5.03-5	1.04-4	2.73-4
Cr-51	5.22-6	3.18-4	1.10-3
Cr-52	3.64-4	7.36-4	9.41-4
Cr-53	1.2-10	6.16-6	1.02-4
Cr-54	1.74-6	2.42-5	1.01-4
Mn-49	0.	1.94-9	9.51-8
Mn-50	1.22-6	6.28-6	7.79-6
Mn-51	1.62-5	6.22-5	2.89-4
Mn-52	1.98-4	5.73-4	7.97-4
Mn-53	6.16-4	8.69-4	2.01-3
Mn-54	1.94-4	1.81-3	3.66-3
Mn-55	5.82-4	1.15-3	1.46-3
Fe-52	5.53-7	8.97-6	2.36-5
Fe-53	1.22-4	1.87-4	2.72-4
Fe-55	5.01-3	7.03-3	8.27-3
Co-53	1.27-7	9.14-7	2.78-6
Co-54	0.	2.69-6	1.55-5
p + COBALT			
neut	1.45-2	2.87-2	4.70-2
H-02	4.49-4	1.26-3	2.45-3
H-03	2.83-5	9.20-5	1.92-4
He-04	1.37-3	2.56-3	4.08-3
Sc-44	0.	0.	7.3-29
Sc-45	0.	5.5-25	2.6-13
Sc-46	0.	8.8-21	1.2-10
Sc-47	2.3-22	6.3-12	7.69-8
Sc-48	0.	0.	3.2-21
Sc-49	0.	9.3-25	1.4-13
Ti-45	0.	0.	3.1-28
Ti-46	0.	1.9-22	1.9-11
Ti-47	3.5-20	2.6-10	4.13-7
Ti-48	5.00-9	1.26-6	1.18-5
Ti-49	0.	2.5-13	6.47-8
Ti-50	1.3-18	3.67-9	9.64-7
Ti-51	0.	0.	7.4-16
Ti-52	0.	5.5-24	3.0-13
V-47	0.	0.	7.5-21
V-48	0.	7.8-19	1.51-9
V-49	1.3-15	1.11-8	3.39-6
V-50	5.3-12	3.50-7	3.43-5
V-51	2.78-7	1.58-5	7.70-5
V-52	0.	4.3-12	2.02-7
V-53	4.5-18	5.77-9	7.57-7
V-54	0.	0.	2.6-20
V-55	0.	0.	1.2-15
Cr-49	0.	2.1-19	7.1-10
Cr-50	1.8-13	1.81-7	9.44-6
Cr-51	7.60-7	2.03-5	7.90-5
Cr-52	2.75-5	5.47-5	1.08-4
Cr-53	2.07-9	6.65-6	8.63-5
Cr-54	1.03-6	1.78-5	5.68-5
Cr-55	0.	3.1-14	8.45-8
Cr-56	8.8-20	3.8-10	1.56-7
Mn-51	0.	0.	2.12-8
Mn-52	0.	1.16-7	1.14-5
Mn-53	3.72-7	7.21-5	5.16-4
Mn-54	4.90-5	4.13-4	9.41-4
Mn-55	7.44-5	1.23-4	1.64-4
Mn-56	1.7-11	3.90-6	5.26-5
Mn-57	1.28-7	4.45-6	1.36-5
Fe-52	0.	0.	9.21-9
Fe-53	0.	9.52-7	3.58-5
Fe-54	9.22-5	4.98-4	9.69-4
Fe-55	5.32-4	7.82-4	1.29-3
Fe-56	6.17-4	1.59-3	3.37-3
Fe-57	3.87-4	1.57-3	2.56-3
Fe-58	5.10-4	8.34-4	1.09-3
Co-54	0.	0.	4.5-11

product	Incident Proton Energy 30MeV	40MeV	50MeV
p + COBALT (Continued)			
Co-55	0.	2.72-6	7.25-5
Co-56	1.30-5	4.05-4	1.16-3
Co-57	1.38-3	3.76-3	5.48-3
Co-58	3.50-3	5.40-3	7.15-3
Ni-56	0.	2.28-6	2.37-5
Ni-57	5.98-5	3.29-4	5.15-4
Ni-58	2.49-3	3.09-3	3.56-3
p + NICKEL			
neut	3.35-3	7.71-3	1.41-2
H-02	2.37-4	7.53-4	1.56-3
He-04	1.10-3	2.38-3	4.20-3
Cr-50	3.6-10	9.87-7	1.56-5
Cr-52	5.7-10	5.12-7	4.72-5
Mn-51	2.39-6	2.22-5	7.69-5
Mn-52	1.3-17	9.41-9	1.56-5
Mn-53	9.36-6	2.86-4	8.28-4
Mn-54	9.1-17	1.35-8	6.48-6
Mn-55	1.01-7	9.78-6	8.79-5
Fe-53	2.50-7	4.09-5	2.29-4
Fe-54	5.75-4	1.02-3	1.22-3
Fe-55	2.05-6	1.86-4	1.43-3
Fe-56	3.61-4	1.59-3	2.87-3
Fe-57	1.7-10	3.81-6	9.28-5
Fe-58	3.30-6	3.39-5	8.41-5
Co-54	9.38-6	9.77-5	3.26-4
Co-55	1.71-4	1.84-4	2.85-4
Co-56	3.16-4	2.02-3	3.89-3
Co-57	3.53-3	5.10-3	6.32-3
Co-58	7.67-5	6.81-4	1.37-3
Co-59	2.87-4	5.36-4	6.77-4
Ni-56	9.60-6	8.23-5	2.17-4
Ni-57	1.17-3	1.84-3	2.29-3
Ni-59	1.31-3	1.87-3	2.23-3
Cu-57	1.22-6	9.72-6	3.10-5
Cu-58	1.39-4	1.61-4	1.77-4
p + COPPER			
neut	1.20-2	2.35-2	3.73-2
H-02	3.12-4	8.62-4	1.68-3
He-04	1.85-3	3.36-3	5.07-3
Fe-55	3.11-8	4.64-6	2.97-5
Fe-56	1.18-5	3.34-5	1.09-4
Fe-57	2.22-8	1.61-6	1.84-5
Fe-58	7.74-7	6.16-6	3.26-5
Fe-59	1.1-16	7.4-10	1.13-7
Fe-60	8.1-12	3.21-9	5.84-8
Co-57	1.95-9	1.16-5	1.20-4
Co-58	2.82-5	3.06-4	7.95-4
Co-59	1.38-4	3.88-4	1.02-3
Co-60	9.20-7	1.66-5	9.11-5
Co-61	2.32-6	1.81-5	9.76-5
Co-62	2.0-17	1.08-9	2.43-7
Co-63	5.6-12	3.25-9	1.01-7
Ni-58	3.30-5	3.09-4	6.87-4
Ni-59	7.29-4	1.01-3	1.14-3
Ni-60	5.76-4	1.22-3	2.50-3
Ni-61	6.96-4	1.94-3	2.85-3
Ni-62	7.52-4	1.14-3	1.50-3
Ni-63	6.37-6	5.53-5	1.08-4
Ni-64	6.69-6	1.40-5	1.98-5
Cu-60	1.8-12	8.57-6	1.59-4
Cu-61	3.95-4	1.71-3	2.51-3
Cu-62	2.41-3	3.30-3	4.22-3
Cu-64	5.68-4	8.82-4	1.13-3
Zn-61	7.26-7	4.12-5	1.88-4
Zn-62	5.96-4	8.09-4	9.08-4
Zn-63	1.34-3	1.82-3	2.36-3
Zn-64	1.32-3	1.59-3	1.72-3
p + TUNGSTEN			
neut	1.97-2	4.45-2	8.02-2
Ta-179	7.2-13	6.76-9	2.46-7
Ta-180	7.1-10	1.13-7	1.61-6
Ta-181	2.83-9	5.57-8	3.64-7
Ta-182	1.87-9	5.28-8	4.41-7
Ta-183	1.19-9	3.84-8	3.07-7
Ta-184	4.1-12	1.61-9	4.09-8
Ta-185	3.6-10	1.57-8	1.65-7
W-178	0.	7.20-7	9.25-5
W-179	1.99-7	5.27-5	3.63-4
W-181	1.34-4	5.01-4	1.18-3
W-185	1.04-4	2.53-4	4.01-4
Re-178	0.	1.61-6	3.94-4
Re-179	1.31-5	7.23-4	2.11-3
Re-180	6.12-4	1.77-3	3.15-3
Re-181	1.70-3	3.32-3	4.49-3
Re-182	1.88-3	2.85-3	4.42-3
Re-183	1.51-3	2.88-3	3.54-3
Re-184	1.28-3	1.62-3	1.78-3
Re-185	7.78-4	8.68-4	9.37-4

*

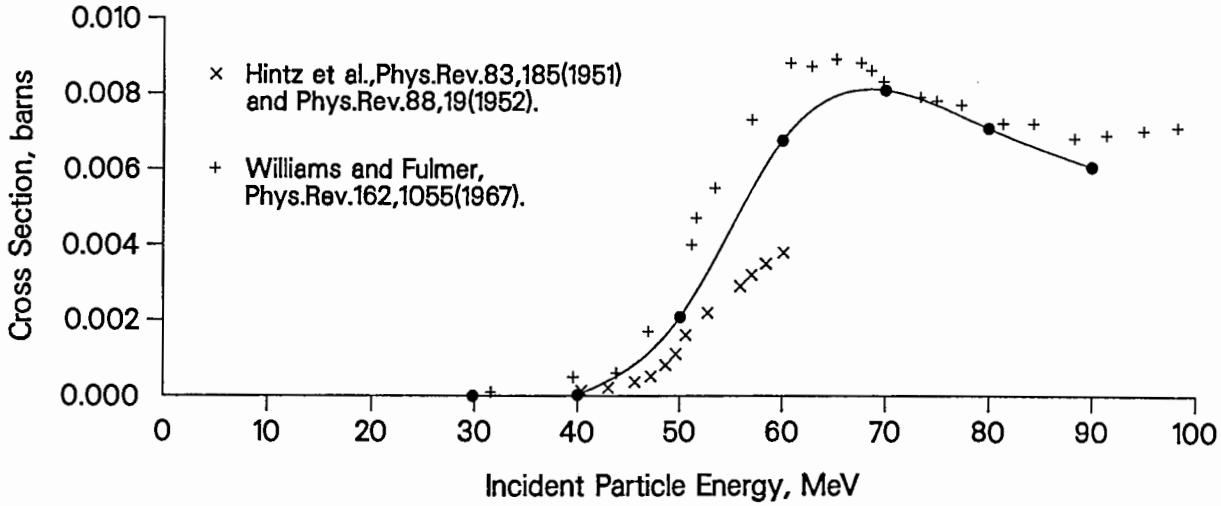

Fig. 1 GNASH results for ^{18}F production from protons on ^{27}Al

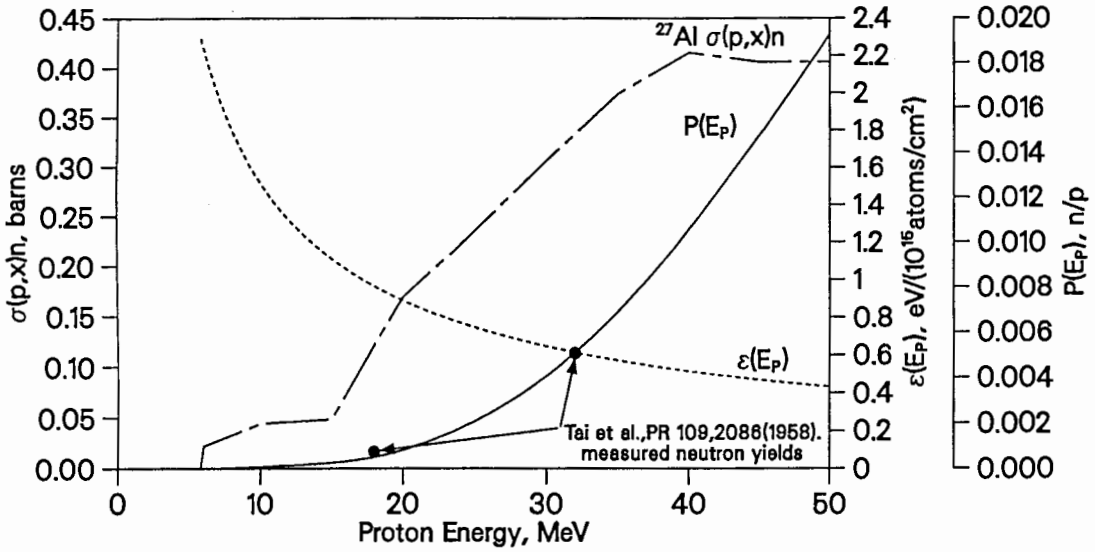

Fig. 2 GNASH-calculated $^{27}Al(p,x)n$ cross section, proton stopping cross section of Al, and calculated p+Al thick target neutron yield.

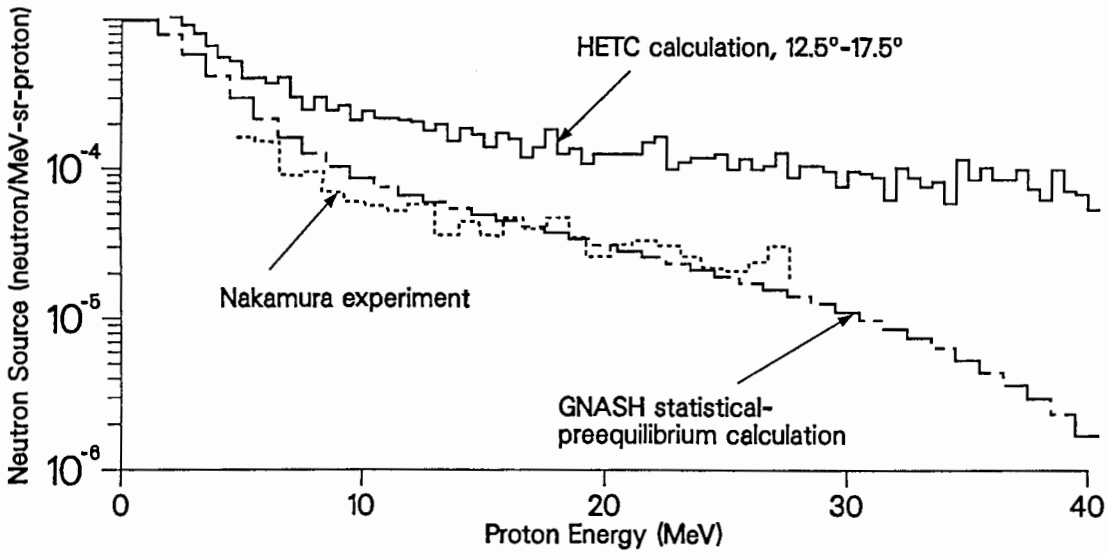

Fig. 3 Comparison of the 52-MeV p+Cu 15° neutron spectrum measured by Nakamura et al. and calculated with GNASH and HETC.